

Polyelectrolyte gels in poor solvent: Equilibrium and non equilibrium elasticity

T.A. Vilgis^(1,2), A. Johner⁽¹⁾, J. F. Joanny⁽¹⁾

⁽¹⁾*Laboratoire Européen Associé, Institut Charles Sadron,
6, rue Boussingault, F- 67083 Strasbourg, Cedex, France*

⁽²⁾*Max-Planck-Institut für Polymerforschung,
Postfach 3148, D-55021 Mainz, Germany*

(October 30, 2018)

We study theoretically using scaling arguments the behavior of polyelectrolyte gels in poor solvents. Following the classical picture of Katchalsky, our approach is based on single chain elasticity but it accounts for the recently proposed pearl-necklace structure of polyelectrolytes in poor solvents. The elasticity both of gels at swelling equilibrium and of partially swollen, non equilibrium, gels is studied when parameters such as the ionic strength or the fraction of charged monomers are varied. Our theory could be useful to interpret recent experiments performed in Strasbourg that show that if identical gel samples are swollen to the same extent at different pH the sample with the highest charge has the lowest shear modulus.

I. INTRODUCTION

Polyelectrolyte gels can absorb a considerable amount of water and swell up to 1000 times. This remarkable property can be monitored by the salt concentration and makes polyelectrolyte gels good candidates for superadsorbent materials. From a fundamental point of view, polyelectrolyte gels are less understood than neutral gels. In some respects, a neutral gel at swelling equilibrium is similar to a semi-dilute polymer solution at the overlap concentration, the mesh size in the gel grows up to the point where the meshes marginally overlap, this is the so-called c^* description. Neutral gels thus benefit to a large extent from the powerful scaling description developed for single neutral chains and solutions. The situation is, however, complicated by trapped entanglements that can, depending on the preparation process, severely restrict swelling and by heterogeneities (fluctuations in the crosslink density) that can be revealed by swelling [1,2].

There is no such strong analogy between polyelectrolyte gels and solutions, mainly because of the long ranged electrostatic interaction and the presence of counterions. Counterions are free in the solution whilst they are trapped in the equilibrium gel (immersed in a large excess of salt-free water) to ensure macroscopic electroneutrality. The osmotic pressure of the trapped counterions, with no counterpart in solution, turns out to be the main reason for swelling. Though it originates from the electrostatic interaction between polymer and counterions this pressure is not electrostatic in nature, it does not depend on the strength of the electrostatic interaction, say on the Bjerrum length. The forces responsible for the swelling may be identified as the electrostatic forces acting on the gel boundary where the counterion concentration vanishes. As often in these matters, the thermodynamic point of view, where the contribution from the narrow non neutral boundary is negligible, is more convenient.

Neutral gels also appear simple in the sense that the chain interactions do not play a major role in the elastic properties. The elastic modulus for unentangled networks for example can be simply determined from the density of crosslinks. Even very refined theories [3,4] show clearly that the modulus for unentangled networks is given by $G = ck_B T/N$, where c is the monomer density and N is the number of monomers of the chain strand between two crosslinks. This simple result is quite independent of solvent quality; the excluded volume interactions influence mainly the bulk properties such as the compression modulus, rather than the shear elastic effects; the shear experiments probe, to first order, the strand elasticity and the shear modulus is proportional to the elastic energy density stored in the gel. The elasticity of polyelectrolyte gels is less simple because the gel structure is not simply that of the polyelectrolyte solution. Due to the stretching by the counterion pressure the shear modulus is actually higher than what would be simply given by the crosslink density; it is further expected to explicitly depend on the charge density, the quality of the solvent and the salt concentration.

In the present paper we are concerned with the behavior of polyelectrolyte gels in poor solvent. Khokhlov and coworkers have studied in details the behavior of such "responsive" gels on the basis of the Flory-Rehner theory, i.e., the additivity of the different parts of the free energy. The starting point of these models is the Gaussian elastic free energy of the neutral networks to which all the other contributions such as, the entropy of the counterions, the electrostatic contributions or the solvent-monomer interactions are added [5].

The aim of the present paper is different. We study the elastic modulus of the polyelectrolyte gel in a poor solvent using the recent work on the conformation of polyelectrolyte chains. Polyelectrolytes in poor solvents are predicted to form pearl necklace structures [6,7]. These structures result from a Rayleigh instability of the collapsed globules

if their radius exceeds a certain size. In a previous paper we have studied the stretching of these pearl necklace structures [8]. We calculated stress-strain relationships in various situations. For chains with many pearls, we found a continuous stress-strain relation. If the necklace has only a few pearls, it stretches discontinuously and the pearls are dissolved one by one.

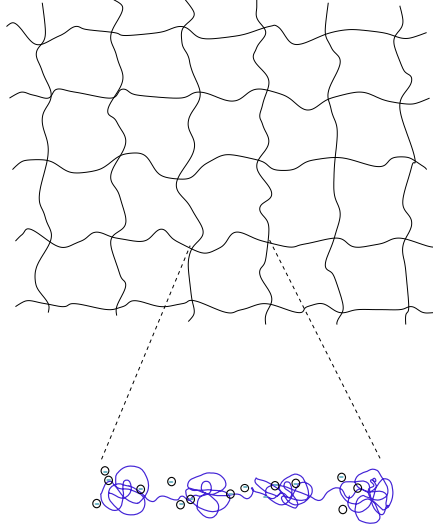


FIG. 1. The model of gel under investigation. The network consists of strands which can be described by polyelectrolyte chains in poor solvent. The strands themselves possess a pearl necklace structure

The model used in the paper below consists of weakly charged crosslinked chains, with N monomers of size b , a fraction f of which are charged. The interaction strength of the Coulomb potential $V(\mathbf{r}) = k_B T l_B / r$ is expressed by the Bjerrum length $l_B = e^2 / (4\pi\epsilon k_B T)$; ϵ is the dielectric constant of the solvent.

The paper is organized as follows: We first summarize the known results on polyelectrolyte gels in θ -solvent and on necklaces [6,8]. We then discuss equilibrium gels and nonequilibrium gels in section III and finally present our conclusions.

II. POLYELECTROLYTE GELS IN θ -SOLVENT AND NECKLACE CONFORMATIONS

In view of the following considerations it is useful to review first the main points of the present state of the art, via simplest scaling arguments. These include the theory of polyelectrolyte gels in θ -solvent [9], the illustration of the role of the counterions, and the necklace description of polyelectrolytes in poor solvents [7,8]. For the latter we are going to discuss single chain elasticity and semi-dilute solutions.

A. Polyelectrolyte gels in θ -solvent

The size of an isolated polyelectrolyte chain in θ -solvent can be estimated from the balance between entropy and electrostatic energy. A weakly charged chain in a θ -solvent stretches provided that the fraction of charged monomers f is large enough, $f > N^{-3/4}$. The conformation remains locally isotropic at scales smaller than the electrostatic blob size

$$R_c = b(l_B f^2 / a)^{-1/3} \quad (1)$$

and the chain is extended at larger length scales. This leads to the usual blob model [10] with an overall radius : $R = bN \left(\frac{l_B f^2}{b} \right)^{1/3}$. In solution, the chains overlap at concentrations c larger than the overlap concentration $c^* = N/R^3$. In a semi-dilute solution ($c > c^*$) the chains make a random walk of step length $\xi_c = (l_B f^2 / a)^{-1/6} (ca^3)^{-1/2} b$ with an overall size

$$R_{1/2} = N^{1/2} (l_B f^2 / b)^{1/12} (cb^3)^{-1/4} b \quad (2)$$

that becomes equal to the gaussian radius at high concentration when the electrostatic blobs begin to overlap at concentrations $c \gg c^{**} \sim f^{2/3}$.

The swelling equilibrium of a charged gel results from a balance between the counterion contribution to the osmotic pressure $\Pi_{\text{counter}} = k_B T f c$ and the elastic contribution $\Pi_{\text{elastic}} = -k_B T c R^2 / N^2 b^2$, the equilibrium meshsize and concentration are:

$$R = N f^{1/2} b \quad c = N^{-2} f^{-3/2} b^{-3} \quad (3)$$

where the so-called c^* theorem $c = N/R^3$ which assumes disentangled meshes is used. The meshsize R is larger than the size of an isolated chain comprising N monomers and does not depend on the Bjerrum length. The contribution of the direct electrostatic interaction to the energy density $F_e = k_B T l_B f^2 N^2 / R^4$ can be checked to be negligible.

The addition of salt in water at low concentrations $n_s < c f$ does not affect the swelling. At higher salt concentrations, however, the gel is expected to deswell, as the small ion contribution to the osmotic pressure in the gel approaches the osmotic pressure in the surrounding bulk solution. The ion partitioning is fixed by a Donnan equilibrium, that fixes the inner salt concentration n_{si} and to the reduced small ion pressure difference $\Delta \Pi_{\text{ion}} = c^2 f^2 / (4n_s)$. This pressure difference is compensated by the elastic contribution of the chains in an equilibrium gel and the concentration is

$$c = N^{-4/5} f^{-6/5} (n_s b^3)^{3/5} b^{-3} \quad (4)$$

It is easily checked that the direct electrostatic energy density remains negligible as long as the mesh is weakly screened $\kappa R < 1$. In the strong screening limit $\kappa R > 1$ the interactions become short-range. If we impose a scaling form $F_e = k_B T (l_B f^2 N^2 / R^4) f(\kappa R)$ and require that the free energy density is quadratic in the polymer charge density we obtain $f(x) \propto x^{-2}$ for the scaling function and the electrostatic free energy F_e is of the same order as $\Delta \Pi_{\text{ion}}$. Equation(4) is thus expected to hold at the scaling level.

B. Necklace structure and elasticity

In a poor solvent a long neutral polymer chain collapses into a dense globule. The poor solvent conditions are characterized by a negative excluded volume $v = -\tau b^3$, where $\tau = (\theta - T)/\theta$ is the relative distance to the Flory compensation temperature θ . In the absence of electrostatic interactions, the chain collapses into a dense globule that may be viewed as a small region of dense polymer phase at co-existence; the finite size of the globule is associated with an extra energy penalty due to the polymer-water surface tension. The balance of the osmotic pressure between the dense and dilute phases (the latter at almost vanishing concentration) yields the concentration inside the globule $c = \tau/b^3$. Alternatively, the dense phase may be described by a close packing of thermal blobs of size $\xi_t = b/\tau$, containing $g = 1/\tau^2$ monomers. A globule of N monomers has then a radius $R = b(N/\tau)^{1/3}$. The corresponding surface tension is $\gamma = k_B T / \xi_t^2 \propto \tau^2 / b^2$.

In a poor solvent, a long polyelectrolyte chain adopts an elongated shape determined by a balance between surface tension and electrostatic self-energy. The first model was proposed by Kokhlov who optimized the free energy of a cylindrical globule to obtain the transverse radius given by the electrostatic blob radius R_c eq.(1), and the length L imposed by the globule volume $V = N b^3 / \tau \sim L R_c^2$. At least at the scaling level, this description holds as long as there is no additional length scale. Recently it was suggested that the charged globule is subject to a Rayleigh instability and splits into connected droplets, the pearls, with a size of order R_c . The polymer strands separating the pearls are stretched due to the electrostatic repulsion. However equilibrium between pearls and strands imposes the strand tension. In a first approximation, the strand tension is the equilibrium tension $k_B T \tau / b$ when a polymer strand is pulled out of the dense equilibrium phase; the strands can then be viewed as linear arrays of Gaussian blobs of size $\xi_t = b/\tau$. Noting that, up to a logarithmic factor, the repulsion between two half-necklaces is the same as the interaction between two adjacent pearls, we find the strand length l and the total chain length L .

$$l = b(b\tau/l_B f^2)^{1/2} \quad L = bN(l_B f^2 / b)^{1/2} \tau^{-1/2}, \quad (5)$$

where we use the pearl mass $m = \tau b / (l_B f^2)$ associated with the radius R_c .

At low charge fraction or/and very poor solvent, the pearl surface potential calculated in the previous picture is larger than the thermal energy. The counterions are regulated by the pearls, this happens for $\tau > \alpha^3 (b f / l_B)^{1/3}$ with $-\alpha k_B T$ the counterion chemical potential. The condensation of counterions inside the globules actually suppresses the Rayleigh instability and a large globule is stable against the necklace.

Added salt at concentration n_s , screens the electrostatic interactions, the screening length κ^{-1} is related to the salt concentration through $\kappa^2 = 8\pi l_B n_s$. The necklace structure itself is only marginally affected as long as the interaction between adjacent pearls is not screened $\kappa l < 1$. For higher salt concentrations however the distance between nearest pearls along the chain is almost fixed at the screening length.

In a salt-free solution, necklaces overlap above the concentration $c^* = N/R^3$ and a single chain can be viewed as a random walk with a step length $\xi_c = (l_B f^2/b)^{-1/4} \tau^{1/4} (cb^3)^{-1/2} b$, independent of the overall chain size, and a radius [7]:

$$R = N^{1/2} (l_B f^2/b)^{1/8} (cb^3)^{-1/4} \tau^{-1/8} b \quad (6)$$

This description holds at moderate concentration as long as there are several pearls per correlation length ξ_c , at higher concentration there remains one pearl per correlation length; we not consider this regime any longer.

When the single necklace is submitted to an external pulling force φ , pearls are progressively dissolved and converted into strand when the force is increased. When there are only a few pearls, each pearl dissolution translates into a length jump under imposed force or a force drop under imposed length. For a higher number of pearls however the pearl number fluctuates by more than one unit, single pearl features are washed out and the force curve is continuous. This is the regime of interest for the gel system where elastically active paths can be quite long. The chain length can be related to the pulling force by a force balance on the half-necklace similar to the one leading to eq.(5) including the external force φ :

$$L(\varphi) = L(0) \left(1 - \frac{\varphi b}{k_B T \tau} \right)^{-1/2} \quad (7)$$

(where all finite size corrections are neglected). The elastic energy stored in the chain is dominated by the stretched strands (provided $L > L(0)$) and is about $k_B T$ per tensile-blob of radius ξ_t . This simple argument fails when most of the pearls are dissolved, i.e. for $L > Nb\tau$. The maximum length (when all pearls are used up) which represents an upper bound for the validity of the continuous model.

III. POLYELECTROLYTE GELS IN POOR SOLVENT

A. Equilibrium gels

We want here to include the details the pearl-necklace structure for the elastic chains of the gel; this cannot be done using complete calculations as for the θ -gel. However, useful predictions can be made at the scaling level. We propose two different models : the c^* -gel where the meshes are disentangled at swelling equilibrium and for which the preparation state is irrelevant, and the affine deformation model where the equilibrium swelling depends on the preparation state. The affine model considers that the deformation of the gel with respect to the preparation state is affine at all length scales; this imposes the constraint that the polymer content of a mesh volume remains constant upon swelling $cL_m^3/N = c_p L_p^3/N = \alpha$ where index p refers to the preparation state. This constraint can be understood as imposing that initially entangled meshes do not disentangle. The special (limiting) case $\alpha = 1$ corresponds to the c^* -gel, obtained here by reacting all temporary contact points between different chains of a semi-dilute solution during the crosslinking process. Higher values of α are obtained if the gel is prepared in a semidilute or a dense solution when only a small fraction of the temporary contact points are crosslinked.

1. c^* -model

The c^* -model is based on the Katchalsky picture [11]. The equilibrium gel is immersed in a solvent reservoir that imposes its osmotic pressure. In the absence of salt (actually if the salt concentration n_s is such that $n_s < cf$), the osmotic pressure in the gel vanishes (it is much lower than the ideal gas counterion pressure $k_B T cf$). The contribution arising from the counterions and from the strand elasticity thus (almost) cancel.

$$\Pi = \Pi_{\text{elastic}} + \Pi_{\text{count}} = 0 \quad (8)$$

The counterion contribution to the osmotic pressure, similar to that for the θ -gel is dominated by the entropic term $\Pi_{\text{counter}} = k_B T cf$. The contribution arising from the strand elasticity can be derived from the elastic energy density that is proportional to the density of tensile-blobs :

$$F_{elastic}/k_B T = (c/N)(N/m)(l/\xi) = \tau/(L_m^2 b) \quad (9)$$

it varies as the $2/3$ power of concentration. As for the θ -gel, we assume that disentangled meshes are at equilibrium, $c = N/L_m^3$. The contribution of the elastic energy to the osmotic pressure $cdF_{elastic}/dc - F_{elastic}$ is negative, and only differs from $F_{elastic}$ by a factor $-1/3$. At the scaling level we thus write

$$\Pi_{elastic}/k_B T = -(c/N)(N/m)(L_m/\xi) = -\tau/(L_m^2 b) \quad (10)$$

This is compensated by the counterion pressure $\Pi_{count} = k_B T c f$ at the gel equilibrium concentration :

$$c = \frac{\tau^3}{N^2 f^3 b^3} \quad (11)$$

where the meshsize is

$$L_m = b f N / \tau \quad (12)$$

It is easily checked that the mesh is stretched with respect to a corresponding free necklace comprising N monomers, and as for a θ -gel, the structure of the gel in a poor solvent is not that of a c^* -solution. On the other hand our description of the stretched necklace requires the necklace to be shorter than a string of thermal blobs as the pearl-necklace description remains valid only if most monomers belong to pearls: $L < N\tau b$. Eq.(12) thus holds for $\tau > f^{1/2}$; closer to the θ -point, the solvent quality becomes irrelevant and the structure is that of a θ -gel. It can actually be checked that the concentration smoothly crosses over with that of the θ -gel when $\tau = f^{1/2}$.

For very poor solvents we know from the single necklace study that the counterions are no longer free and condense on the pearls. The gel then macroscopically collapses, this happens for

$$\frac{l_B \tau^3}{b f} > \left(\log \frac{N^2 f^2 b^3}{\tau^3} \right)^3 \quad (13)$$

where the logarithm accounts for the counterion entropy at the onset of condensation. Qualitatively, the gel is collapsed for $\tau > f^{1/3}$. In summary, the poor solvent conditions are irrelevant close to the θ -point as long as $\tau < f^{1/2}$, the gel shrinks continuously for intermediate solvents $f^{1/2} < \tau < f^{1/3}$ and undergoes collapse at $\tau \sim f^{1/3}$ due to counterion condensation. This behavior is represented in FIG (2).

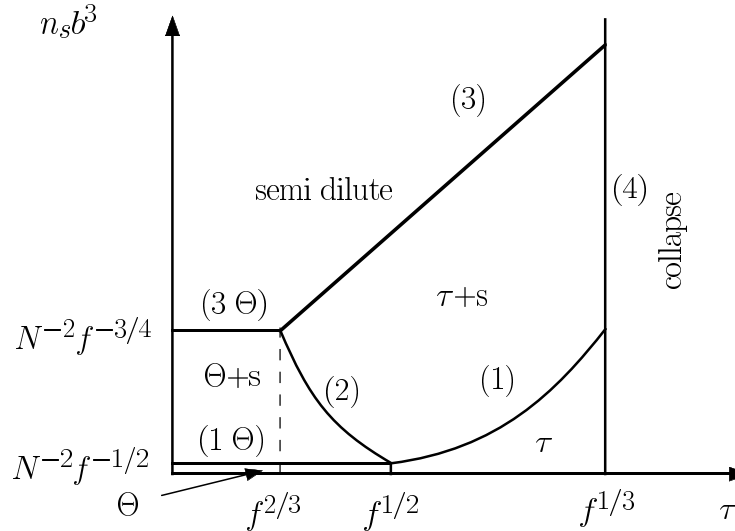


FIG. 2. The phase diagram of the gel as a function of salt content and solvent quality, see text

The compression modulus and the shear modulus of the equilibrium gel, are proportional to the counterion free energy density and to the elastic energy density respectively, and are of the same order at equilibrium:

$$G \propto K \propto \Pi_{\text{count}} = \frac{k_B T}{N^2 f^2} \left(\frac{\tau}{b} \right)^3 \quad (14)$$

When monovalent salt is added to the bulk solution, a Donnan equilibrium fixes the inner salt concentration and the small-ion excess pressure. For salt concentrations n_s smaller than the bound charge concentration cf , salt is irrelevant, and the small ion excess pressure remains equal to $k_B T cf$. For $n_s > cf$ in contrast, the small ions contribute a smaller inner pressure excess $\Delta\Pi_{\text{ion}} = k_B T c^2 f^2 / (4n_s)$.

This osmotic pressure difference is compensated by the elastic contribution given by eq.(10) at the equilibrium meshsize and concentration:

$$L_m = \frac{N^{1/2} f^{1/2}}{\tau^{1/4} (n_s b^3)^{1/4}} b \quad c = \frac{\tau^{3/4} (n_s b^3)^{3/4}}{N^{1/2} f^{3/2} b^3} \quad (15)$$

At low salt concentration $n_s b^3 < N^{-2} f^{-1/2} (\tau/f^{1/2})^3$ these results crossover the salt-free results eqs.(11,12), line (1) in the diagram FIG (2). Close to the θ -point, $n_s b^3 < N^{-2} f^{-1/2} (\tau/f^{1/2})^{-5}$ the negative excluded volume becomes irrelevant and the results crossover to those obtained for a θ -gel, line (2) in the diagram. The weak screening regime described by eq.(15) is also bound at high salt concentrations : the screening length due to the added salt becomes shorter than the meshsize for $n_s b^3 = \tau b^2 l_B^{-2} N^{-2} f^{-2}$; at higher salt concentration the salt imposes the screening length, line (3) in the diagram. On this line, the electrostatic interaction between polymer strands in the mesh contributes as much as the small-ions to the excess pressure. The crosslinks are thus only marginally relevant. One easily checks that the mesh size is indeed equal to the size of a free strand of mass N . This means that, at the scaling level, there is no difference between the structure of the gel and that of a semi-dilute solution above line (3). Lines (2) and (3) meet at point $B(\tau = f^{2/3} (l_B/b)^{1/3}, n_s b^3 = f^{-4/3} N^{-2} (b/l_B)^{5/3})$. For poorer solvents $\tau > f^{1/3}$, the small ions condense on the pearls and the gel collapses, line (4) in the diagram; this line has not been drawn precisely, in particular the condensation threshold weakly depends upon the salt concentration n_s .

2. The affine deformation model

The condition that the meshes only marginally overlap at swelling equilibrium is now released and replaced by the more general condition of affine deformation $cL_m^3/N = \alpha$ where the constant α is determined in the preparation state. As explained earlier, the physical content of this assumption is quite opposite to that of the c^* -model. The c^* -model is nonetheless recovered in the special case $\alpha = 1$ corresponding to a semi-dilute solution where all temporary contact points between different chains have been made permanent by the crosslinking reaction. In practice $\alpha > 1$ reaches its highest value $N^{1/2}$ for crosslinking in the neutral melt. The elastic energy density now depends on the preparation state through the parameter α .

$$F_{el} = (c/N)(L_m/\xi_{th}) = \frac{\tau\alpha}{bL^2} = \frac{\tau}{b} \left(\frac{c}{N} \right)^{2/3} \alpha^{1/3} \quad (16)$$

The equilibrium meshsize and concentrations have to be modified accordingly and typically differ from those in the c^* -model by a power of α .

For weakly entangled preparation states $1 < \alpha < f^{-1/3}$ the topology of the diagram of states presented in FIG.(2) is preserved. The salt concentration on dividing lines (1), (1 θ) and (2) is increased by a factor α whilst it is decreased by a factor $1/\alpha$ on line (3) and by a factor $\alpha^{-2/3}$ on line (3 θ). The points where these lines cross are shifted as shown in FIG.(3).

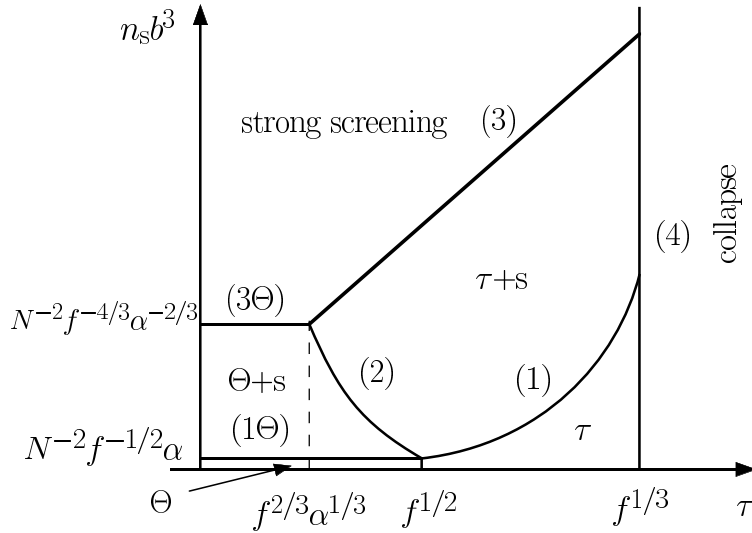


FIG. 3. Phase diagram of the affine model. The general topology is preserved, see FIG.(2), but the axis are shifted and the ranges of the regimes are changed (see text).

As a consequence the parameter range of the intermediate regimes $\theta + S$ and $\tau + S$ is reduced. For somewhat more entangled preparation states $f^{-1/3} < \alpha < f^{-1/2}$, lines (1) and (3) cross: For poor enough solvent $\tau > 1/\alpha$, strong screening occurs before the Donnan effect is relevant as shown on FIG(4).

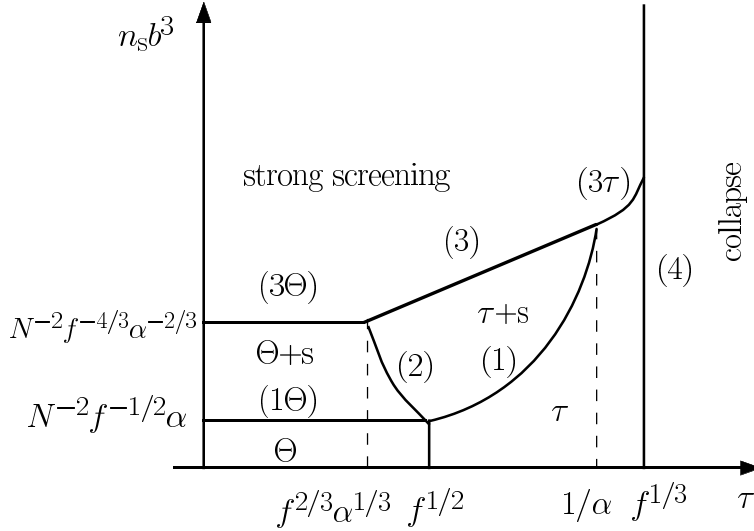


FIG. 4. The phase diagram for poorer solvent, $\tau > 1/\alpha$. The strong screening regime occurs before the Donnan effect is relevant (see text).

In this poor solvent regime a new dividing line (3 τ) directly separates the strongly screened region from the τ region where salt is irrelevant. On this line $n_s b^3 = b\tau^2/(l_B N^2 f^2)$. There is direct contact between the strong screening and the salt irrelevant region over the whole τ -range for $\alpha = f^{-1/2}$ (see figure 3). For higher values of α the remaining lines (3) and (3 θ) no longer shift with α .

The expression of the gel equilibrium concentration and elastic modulus in the various regimes are summarized in table I. Let us stress that for $\alpha > 1$, the gel structure on lines (3) is not that of the solution at the same concentration.

regime	L_m/b	cb^3	$Gb^3/k_B T$
θ	$N\sqrt{f}$	$\alpha N^{-2} f^{-3/2}$	$\alpha N^{-2} f^{-1/2}$
$\theta + \mathbf{S}$	$\alpha^{1/5} f^{2/5} N^{3/5} (n_s b^3)^{-1/5}$	$\alpha^{2/5} f^{-6/5} N^{-4/5} (n_s b^3)^{3/5}$	$\alpha^{4/5} f^{-2/5} N^{-8/5} (n_s b^3)^{1/5}$
τ	$N f \tau^{-1}$	$\alpha \tau^3 N^{-2} f^{-3}$	$k_B T \alpha \tau^3 N^{-2} f^{-2}$
$\tau + \mathbf{S}$	$\alpha^{1/4} f^{1/2} N^{1/2} \tau^{-1/4} (n_s b^3)^{-1/4}$	$\alpha^{1/4} f^{-3/2} N^{-1/2} \tau^{3/4} (n_s b^3)^{3/4}$	$\alpha^{1/2} f^{-1} N^{-1} \tau^{3/2} (n_s b^3)^{1/2}$

TABLE I. Meshsize L_m , gel concentration c and modulus G in the various regimes

B. Shear modulus of non equilibrium gels

When a small amount of water is added to the gel, the added amount imposes the volume and the gel is not at swelling equilibrium. In this case the preparation state is of importance. Most of the (elastic) properties depend on the preparation state [2,3,12]. Rather sophisticated theories have been developed for gels that have not reached swelling equilibrium, but here we argue on a much simpler level. The counterion contribution to the osmotic pressure is given as above by the ideal gas law. We can therefore conclude that the compression modulus is of the order of $k_B T c f$ with c the actual gel concentration. The shear modulus on the other hand, depends on both the preparation state (crosslink configuration) and the swelling state. For a sake of simplicity it is assumed that the gel deforms affinely, and the preparation state is assumed to be an undeformed isotropic state. Thus the measure of the affine deformation with respect to the preparation size is determined by the ratio $\lambda = (c_p/c)^{1/3}$, where c_p and c are the initial and final gel concentrations, respectively. To estimate the elastic energy density stored in the gel we take the semidilute solution at the same concentration c where the chains are stress free as a reference state. At high enough concentration, the elastic chains of the gel have gaussian statistics at large length scale and behave as stretched Gaussian chains of blobs of radius λR_p . The modulus can be written as

$$G = \frac{k_B T c}{N} \left(\frac{\lambda R_p}{R} \right)^2 \quad (17)$$

where R is the equilibrium radius of a chain in a semidilute solution at the same concentration. For moderate concentrations, $c < (l_B/b)^{1/2} f \tau^{-1/2} b^{-3}$, several pearls are found in one correlation length $\xi_c = (l_B f^2/b)^{-1/4} \tau^{1/4} (cb^3)^{-1/2}$ and the chain radius is given by equation 6. We find then for the shear modulus

$$G \propto k_B T \left(\frac{\tau}{f^2} \right)^{1/4} c^{5/6} \quad (18)$$

where the dependence upon the preparation state has been dropped. This analysis is valid in the weak stretching limit where the gel strand is not stretched. For more swollen gels, $c < c_1$, the radius of an elastic chain $R_c = R_p (c/c_p)^{-1/3}$, becomes larger than the radius of an isolated necklace given in eq.(5). The crossover concentration c_1 depends explicitly on the preparation state. For $c < c_1$, the shear modulus is dominated by the overstretched elastic chains and one should use the elastic free energy of equation 16

$$G = k_B T c^{2/3} c_p^{1/3} \tau R_p / (N b) \quad (19)$$

Formally the modulus exhibits a sharp jump at the concentration c_1 within the scaling picture. Around c_1 a more careful consideration of the single chain elasticity is needed. This could be done using a non gaussian elasticity model such as the Langevin model for the chain of blobs, we are reluctant to include it in our rough scaling analysis.

Within the affine deformation model the equilibrium swelling concentration given by $G = c f$ depends explicitly on the preparation state, i.e.,

$$c_{eq} = c_p R_p^3 \left(\frac{\tau}{N f} \right)^3 \quad (20)$$

in contrast to the c^* -model. The two approaches only agree if the initial semi-dilute solution is cross-linked at all the contact points, where the c^* -theorem is indeed expected to apply. In that case, $c_p R_p^3 = N$ and eqs.(20,11) coincide. With this preparation state, the shear modulus of a gel that has not reached equilibrium reads:

$$G = k_{\text{B}}T \left(\frac{c}{N} \right)^{2/3} \frac{\tau}{b} \quad (21)$$

Our results can be tested experimentally by checking the final charge fraction (or temperature) dependence of the shear modulus for identical preparation states. Such experiments, where the shear modulus was indeed found to decrease with the charge fraction at fixed final density, were performed in the group of J.Candau in Strasbourg [13]. One should note however that the experiments were done with annealed polyelectrolytes by monitoring the final charge with the pH of the solution. Annealed polyelectrolytes, as shown recently [14], if the solvent quality is too low can undergo a sharp transition from a collapsed state to a stretched state without any intermediate regime of stable necklace. Our results would thus based on the pearl-necklace conformation would only be useful if the solvent is not too poor which might be the case for polyacrylic acid gels.

IV. CONCLUSION

In this paper we have studied the elastic behavior of polyelectrolyte gels in poor solvent which is markedly different from that of polyelectrolyte gels in good solvent. The study of the single chain behavior already illustrates the different physical behaviors. The stretching of polyelectrolyte chains in a good solvent can be carried out via a simple blob analysis, as the undeformed state of the chains can be described as an extended chain of electrostatic blobs. In a poor solvent, the undeformed chains are composed of pearls and strings. The pearls act as a "reservoir" of monomers which can be pulled out at relatively small forces. In the continuum limit the force increases gently with the deformation. In the case of a low number of pearls, we expect length jumps that correspond to single pearl unwinding at an imposed force. These jumps are rounded by thermal fluctuations in many instances.

For a polyelectrolyte network, we do not expect any force jumps as the elastic chains carrying the stress are much larger than a single mesh; the continuous description is thus appropriate. A gel at swelling equilibrium in a large excess of θ -solvent is known to swell [9] under the effect of the trapped counterion pressure. Most polyelectrolytes however have hydrophobic backbones and the interplay between short range attractions and electrostatics, that leads to the pearl-necklace conformation, is expected to be important as well. Close to the θ -point, for $\tau < f^{1/2}$, the solvent quality is irrelevant and $c \propto f^{-3/2}$. Note that the crossover between the θ -solvent and the poor solvent behavior is different for the equilibrium gel and for isolated chains ($\tau > f^{2/3}$). For intermediate solvent quality $f^{1/2} < \tau < f^{1/3}$ the gel deswells and $c \propto (\tau/f)^3$. When the solvent is very poor $\tau \sim f^{1/3}$, the counterions condense on the pearls and the gel collapses.

When salt is added to the bulk solution, the gel shrinks. The various swelling regimes are represented on the diagram of Fig.(2). If the salt concentration is smaller than counterion concentration in the gel, the effect of salt is negligible. At higher salt concentration, the concentration in the gel increases as $c \propto n_s^{3/4}$. At salt concentrations higher than $\sim \tau/(N^2 f^2)$, the gel has shrunk to the extent that junction points no longer play any role, the properties of the gel are similar to those of a semi-dilute polyelectrolyte solution (the details of this description remain controversial). In all the equilibrium swelling regimes the compression and shear moduli are roughly proportional to each other and to the small-ion excess pressure. The modulus is independent of the strength of the electrostatic interactions, say of the Bjerrum length.

In the more realistic affine deformation model, the equilibrium swelling depends upon the preparation state through the constant $\alpha = cL_m^3/N$ measuring the degree of mesh entanglement. The affine deformation constraint imposes that α remains constant during the swelling i.e., that the polymer content of a mesh volume remains constant and that meshes do not disentangle. The diagram of states is qualitatively similar to that obtained from the c^* -model, meshsizes, the scaling laws for the equilibrium concentration and the elastic modulus are shifted by a power of α with respect to that obtained for the c^* -gel that corresponds to $\alpha = 1$. The results are summarized in table I. For higher degrees of entanglement, $f^{-1/3} < \alpha < f^{-1/2}$, the diagram qualitatively changes: For poor enough solvent $\tau > 1/\alpha$ there is a direct separation line between the salt irrelevant regime and the strong screening regime. For $\alpha > f^{-1/3}$ this happens for any solvent quality.

A small amount of added solvent controls the gel volume, and the swelling remains below the equilibrium swelling. The compression and shear moduli are no longer proportional to each other, even can show opposite variations with the charge fraction. Similar results were obtained previously for the θ -gels [15] and observed in experiments [13]. We find a shear modulus $G \propto (\tau/f^2)^{1/4} c^{5/6}$, that is shear softening upon charge increase when all other parameters are kept constant.

Our picture relies on a scaling description that allows us to account for the essential physics. Some additional subtle effects may arise from the long range character of the electrostatic interaction and its variation with the salt concentration. For gels in a good solvent [15] it has been suggested recently [16,17] that the elastic modulus could

depend on the strength of the interaction and the range of the Debye - Hückel potential at least in some parameter range. Our rough approach would not capture those subtle effects.

Acknowledgments

TAV acknowledges the financial support of the LEA. The warm hospitality of the Institut Charles Sadron is gratefully appreciated.

- [1] J. Bastide, L. Leibler, and J. Prost, , *Macromolecules* **23**, 1821 (1986).
- [2] S. V. Panyukov and I. Rabin, *Rep. Prog. Phys* (1998).
- [3] S. F. Edwards and T. A. Vilgis, *Rep. Progr. Phys* **51**, 243 (1988).
- [4] S. Panyukov, *Sov. Phys. JETP* **71**, 372 (1990).
- [5] A. Khokhlov, S. Starodubtzev, and V. Vasilevskaya, *Adv. Polym. Sci.* **109**, 123 (1993).
- [6] A. V. Dobrynin, M. Rubinstein, and S. P. Obukhov, *Macromolecules* **29**, 2974 (1996).
- [7] A. V. Dobrynin and M. Rubinstein, *Macromolecules* **32**, 915 (1999).
- [8] T. Vilgis, A. Johner, and J. Joanny, *E.P.J. E* (2000).
- [9] J. Barrat, J. Joanny, and P. Pincus, *J. Phys. II France* **2** , 1531 (1992).
- [10] P. G. de Gennes, P. Pincus, R. M. Velasco, and F. Brochard, *J. Phys. (France)* **37**, 1461 (1976).
- [11] A. Katchalsky, S. Lifson, and H. Eisenberg, *J. Polym. Sci.* **7**, 571 (1951).
- [12] R. T. Deam and S. F. Edwards, *Phil. Trans. R. Soc. London Ser. A* **280**, 317 (1976).
- [13] R. Skouri, F. Schosseler, J. P. Munch, and S. J. Candau, *Macromolecules* **28**, 197 (1995).
- [14] M. Castelnovo, P. Sens, and J.-F. Joanny, *Eur. Phys. J. E*, **1**, 115 (2000).
- [15] M. Rubinstein, R. H. Colby, A. V. Dobrynin, and J.-F. Joanny, *Macromolecules* **29**, 398 (1996).
- [16] J. Wilder and T. Vilgis, *Phys. Rev. E* **57**, 6865 (1998).
- [17] T. Vilgis and J. Wilder, *Comp. Theor. Polym. Sci.* **8**, 61 (1998).